Application of vibrational microspectroscopy to biology and medicine

Bhawana Singh[1], Rekha Gautam[1], Srividya Kumar[1], B. N. Vinay Kumar[1], Upendra Nongthomba[2], Dipankar Nandi[3], Geetashree Mukherjee[4], Vani Santosh[5], Kumaravel Somasundaram[6] and Siva Umapathy[1,*]

[1]Department of Inorganic and Physical Chemistry, [2]Department of Molecular Reproduction, Development and Genetics, and
[3]Department of Biochemistry, Indian Institute of Science, Bangalore 560 012, India
[4]Kidwai Memorial Institute of Oncology, Bangalore 560 029, India
[5]National Institute of Mental Health and Neuro Sciences, Bangalore 560 029, India
[6]Department of Microbiology and Cell Biology, Indian Institute of Science, Bangalore 560 012, India

Vibrational microspectroscopic (Raman and infrared (IR)) techniques are rapidly emerging as effective tools to probe the basic processes of life. This review mainly focuses on the applications of Raman and IR microspectroscopy to biology and biomedicine, ranging from studies on cellular components in single cells to advancement in techniques for *in vitro* to *in vivo* applications. These techniques have proved to be instrumental in studying the biological specimen with minimum perturbation, i.e. without the use of dyes and contrast-inducing agents. These techniques probe the vibrational modes of the molecules and provide spectra that are specific to the molecular properties and chemical nature of the species.

Keywords: Biomedical applications, chemometrics, Raman and infrared microspectroscopy, vibrational spectroscopy.

Introduction

VIBRATIONAL microspectroscopic techniques like Raman and infrared (IR) are rapidly gaining ground in modern research. These techniques have been useful to understand a wide variety of interesting basic and applied concepts, ranging from their applications in material characterization to biomedicine. Vibrational spectroscopy facilitates monitoring of bond vibrations as a consequence of interaction of light with the sample. Vibrational spectra are molecule-specific and unique to the nature of the specimen. Importantly, biological materials like proteins, carbohydrates, lipids, nucleic acids, etc. have unique structures and therefore unique spectral fingerprints could be obtained for these molecules. Vibrational spectroscopic techniques have an immediate appeal in the field of biology and medicine because of their fast and non-invasive nature. These techniques allow easy visualization of cellular components based on their intrinsic properties and chemical composition, and provide a potential route to obtain diagnostic markers for diseases.

Background

In vibrational spectroscopy, a small region of the electromagnetic spectrum (EMS) is used, i.e. ultraviolet (UV), visible or IR radiations. However, since long, EM waves (gamma rays to radio waves) have been utilized for various biomedical applications (Figure 1). Various regions of the EMS differ in their wavelengths, which in turn allow us to study various properties of matter. When an

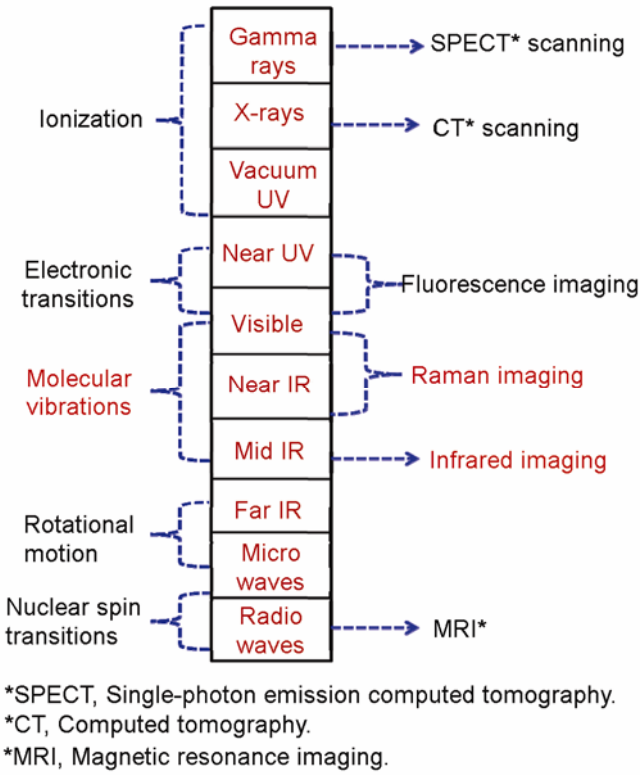

Figure 1. Electromagnetic spectrum and medical imaging modalities.

*For correspondence. (e-mail: umapathy@ipc.iisc.ernet.in)

EM wave strikes an object, the energy of the waves can be absorbed, transmitted, reflected or scattered by the object. One of the widely known uses of radio waves in EMS is magnetic resonance imaging (MRI). Visible light has been popularly used for light microscopy techniques to view unstained, stained or fluorescent samples. Importantly, most of the pathological inferences rely on light microscopy. Fluorescence microscopy has become one of the most widely used techniques, especially for probing specific targets and dynamic processes in chemically fixed or living cells. It has dramatically improved our understanding of the living systems. Although, UV spectroscopy has found limited use in biomedicine, it has been primarily used as a preliminary examination technique for a large number of experiments such as determination of absorption of amino acids (tryptophan), proteins or other biologically important species. The most important application of X-rays in biomedicine is to image bones and tissues. Apart from this, X-ray diffraction has revolutionized the field of protein crystal structure determination. The high-energy gamma rays have been used for single-photon emission computed tomography (SPECT) scanning and positron emission tomography (PET) imaging.

The earliest use of vibrational spectroscopic techniques for probing biomolecules started in the 1940s. Blout and Fields[1], and Elliott and Ambrose[2] recorded the initial vibrational spectra of nucleic acids and proteins respectively. These techniques are sensitive to the changes in the structure, biochemical composition and quantity of cellular components as a consequence of disease, injury or induced stress, and hence act as indicators of diseased or stressed state. At present, vibrational spectroscopy has grown to the status where *in vivo* applications have been carried out[3].

Principle and instrumentation of vibrational spectroscopy

Vibrational spectroscopic techniques, Raman and IR, probe the molecular vibrations (stretching and bending) that are specific to composition and structure of the samples. Raman spectroscopy is based on the principle of inelastic scattering of light by the probed molecules, whereas IR spectroscopy is an absorption-based technique. Raman and IR transitions are complementary to each other. The molecular vibrations which lead to change in the dipole moment are IR-active, whereas the vibrations which lead to change in the polarizability of the molecule are Raman-active.

Raman and IR microspectroscopic techniques are relatively new, wherein spectrometers are coupled with an optical microscope. The microscope allows easy visualization of small species and in the case of heterogeneous samples, the area of interest can be focused and probed selectively.

Raman microspectroscopy

In 1928, C. V. Raman, demonstrated the concept of inelastic scattering of photons on interaction with matter. The frequency of the emitted photons is shifted to a lower or higher value in comparison with the frequency of the incident photons, and this phenomenon is called the Raman effect. The photons that take up energy from the vibrations of the molecule give rise to anti-Stokes signal, whereas photons that give energy to the vibrations of the molecule lead to Stokes signal, as depicted in Figure 2. Raman scattering is a weak effect and is frequently masked by fluorescence. Biological samples are often fluorescent and pose a great challenge in recording Raman spectra. The use of longer probe wavelength in comparison to shorter wavelength not only reduces fluorescence, but also minimizes the sample damage due to lower energy.

Schematic representation of a Raman microspectrometer is shown in Figure 3. It has four main components: (1) laser source, (2) microscope, (3) spectrometer and (4) detector. Laser is a monochromatic light source and at present, it is the most commonly used source for Raman experiments. The selection of the laser wavelength depends on the sample under study. For example, most of the biological samples are preferably probed by long wavelengths. The laser line is directed towards the microscope using various optics and focused onto the sample. In general, the Raman microspectrometer works with back scattering (180°) geometry, i.e. illumination of the sample as well as collection of scattered light from the sample are carried out by the same objective. The objective used determines the spatial resolution, which depends on its numerical aperture (NA). In simplified form, the diffraction-limited spatial resolution can be defined as:

$$R = \frac{\lambda}{2\mathrm{NA}},$$

where $\mathrm{NA} = \eta \sin\theta$, η is the refractive index of the medium between the objective and sample under study,

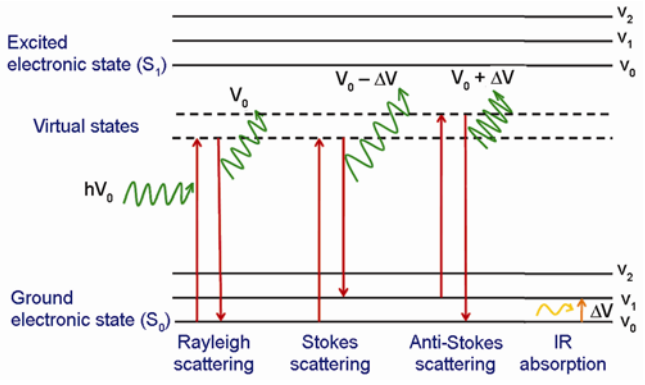

Figure 2. Energy-level diagram representing Raman and infrared processes.

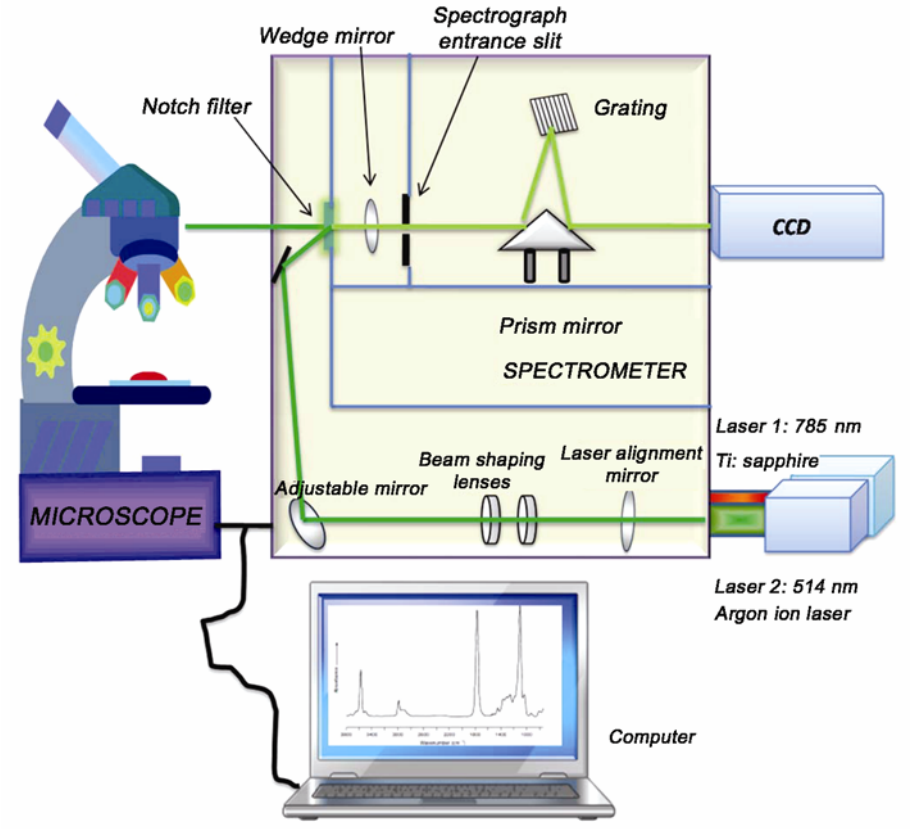

Figure 3. Ray diagram of Raman microspectrometer.

θ the half of the maximum cone angle of light that can enter or exit the lens and λ the wavelength of the incident light.

Smaller the value of R, better will be the spatial resolution. The above equation indicates that as NA increases the spatial resolution improves. Generally, the objectives used are dry objectives, i.e. air serves as the medium between the sample and objective lens. Therefore, the maximum value of NA cannot exceed 1 as the refractive index of air (η_{air}) is 1 and hence limits the spatial resolution. The spatial resolution can be improved further by using water ($\eta_{water} = 1.3$) and oil ($\eta_{oil} = 1.5$) immersion objectives. Furthermore, confocal arrangement can be used to improve the depth resolution (z-direction). In the confocal set-up, a pinhole is placed in front of the detector. This arrangement excludes light from features above or below the object plane within the sample and hence improves depth resolution. Confocal arrangement also improves the signal-to-background ratio by diminishing fluorescence as the sample volume detected at a time is much smaller than the conventional arrangement.

The scattered light collected from the sample enters the spectrometer via a notch filter which is used to filter Rayleigh scattering. The most important component of a spectrometer is the dispersive element (i.e. grating) which decides the spectral resolution. Spectral resolution of a spectrometer is defined as the ability to distinguish between adjacent spectral features in a spectrum. It is a complex function of resolving power of the grating, pixel width and slit width. The linear dispersion of a diffraction grating is directly proportional to the distance between rulings on the grating, i.e. the number of lines per millimetre. The reciprocal of linear dispersion is given by:

$$\frac{d\lambda}{dl} = \frac{d\cos\theta}{mF},$$

where d is the distance between lines on the diffraction grating, m the diffraction order, F the focal length of the focusing mirror, and θ the angle of diffracted light leaving the grating with respect to grating surface normal.

As the number of lines per millimetre of a grating increases, the resolving power of the spectrometer increases. For example, a grating with 1800 lines/mm will resolve adjoining components in a spectrum better than grating with 1200 lines/mm. Finally, the dispersed light is focused onto the charge coupled device (CCD), which is commonly used to detect Raman signals[4].

IR microspectroscopy

Schematic representation of an IR microspectrometer is shown in Figure 4. It also has four major components: (1)

IR source, (2) interferometer, (3) microscope and (4) detector. In contrast to the laser source used in Raman microspectrometer, broadband IR sources are used in this technique (SiC or Globar filament). In the Michelson interferometer, a KBr beam splitter directs the IR broadband radiation coming from the source towards two perpendicularly placed mirrors. One of the mirrors is kept stationary and the other is allowed to move in order to obtain the interference pattern. The interferogram so obtained is Fourier transformed into the IR spectrum. Depending upon the sample condition and data requirement, different sampling modes could be employed for data acquisition such as transmission mode, reflection mode, transflection (transmission-reflection) mode, ATR mode, etc. In the case of transmission and transflection modes, sample thickness plays a deciding role as the IR radiation must pass through the sample, whereas in other modes such as reflection, ATR and grazing angle modes, sample thickness does not restrict the data collection.

IR radiations are detected using mercury cadmium telluride (MCT), deuterated triglycine sulphate (DTGS) or indium antimonide (InSb) detectors, depending on the IR range to be detected. Single-element detectors could be used for spectral data collection as well as for mapping experiments. The focal plane array detector (FPA) is a two-dimensional arrangement of many such small detectors (pixels), which provides the spectral and spatial information simultaneously. Global imaging experiments can be carried out using FPA detectors. Although mapping experiment also provides the same kind of information, the time taken by such an experiment is usually more. In the case of mapping experiment, the data are collected point by point in a sequential manner rather than simultaneously as in case of global imaging using a FPA detector[5].

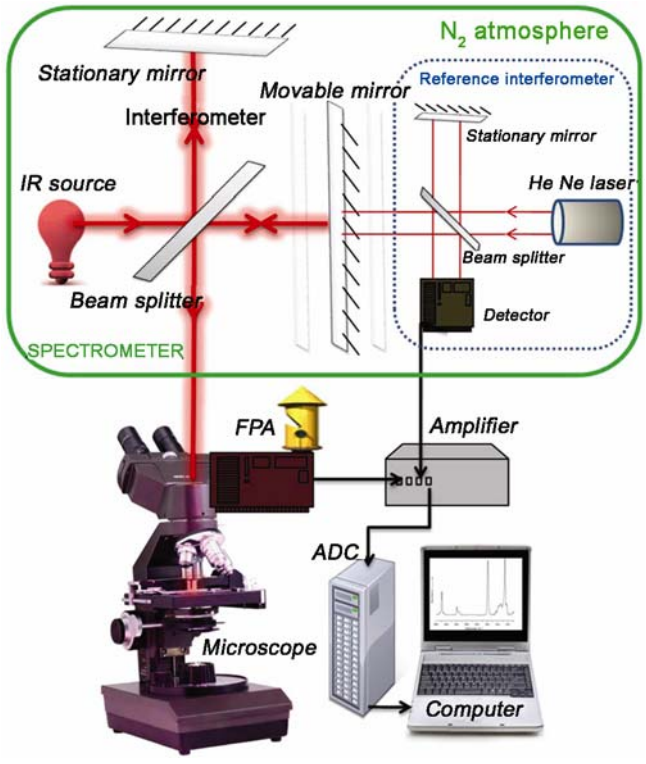

Figure 4. Ray diagram of FTIR microspectrometer.

Applications of vibrational spectroscopy

Numerous applications of Raman and IR microspectroscopy have been reported in the literature to address key questions in biology. Some of these applications have been discussed below.

Vibrational spectroscopy of tissues

Raman and IR techniques are particularly attractive as they provide biochemical information without the requirement of external contrast-inducing agents. In spite of widespread use of instrumental techniques like MRI, PET, X-ray, etc. conventional histopathological identification of diseased tissues by morphological pattern recognition remains the gold standard. The major drawbacks of the histopathological assessment are delays in diagnosis and interpretational variations among the pathologists. There are number of reports where systematic studies have been carried out to assess inter-observer diagnostic variability[6]. Therefore, among the medical community, increasing requirement has been felt for interdisciplinary approaches to improve the diagnostic potential of 'difficult to determine cases' in a shorter time-frame. Therefore, for precise and rapid diagnosis it is essential to utilize and develop new methodologies in conjunction with the existing methods.

Vibrational microspectroscopy coupled with advanced computational methods proves to be a potential tool for detecting different clinical disorders like cancer, cataract sclerosis, etc. The benign and malignant forms of prostate, breast, colon, cervical and brain cancer have been widely studied by Raman and IR techniques[7]. These techniques have also been used to monitor modifications in the bone and other mineralized tissues in terms of developmental changes, detection of disease and drug-induced changes[8]. FTIR ATR microspectroscopy has been used to determine conformational changes in protein and lipid structures[9]. Itte *et al.*[10] have used confocal Raman microspectroscopy to analyse the secondary and tertiary conformational changes in the human lens protein (crystallins) with age.

Recently, FTIR imaging has been used to analyse the changes occurring in multiple sclerosis. Minute chemical and structural changes were observed by FTIR microscopy, which were not observed by conventional histology. This study helped in understanding the neuropathology of the disease more specifically and also

the mechanism of lesion formation[11]. Yang *et al.*[12] have shown the potential of FTIR imaging in biomedical applications by demonstrating the mapping of biochemical changes in myocardial infarction. IR spectroscopy has been used to identify biochemical changes in endometrial tissues growing outside the uterus (ectopic)[13]. Raman microspectroscopy has been used for the chemical analysis of individual cellular and extracellular components in atherosclerotic lesions. This study helped to analyse the morphologic composition of atherosclerotic coronary artery lesions[14]. Peter *et al.*[15] have shown that confocal Raman microspectroscopy could be used for *in vivo* study to monitor the molecular concentration profiles in the skin. They used the technique to determine the water concentration in the stratum corneum as a function of distance to the skin surface and also determined the concentration of constituents like serine, glycine, pyrrolidone-5-carboxylic acid, arginine, ornithine, citrulline, alanine, histidine, urocanic acid, lactates and urea[15]. Bakker *et al.*[16] studied classification of normal and dysplastic tissues (*in vivo*) using fibre-optic probes coupled with Raman spectrometer and were able to distinguish between normal tissue, low-grade dysplasia and high-grade dysplasia/carcinoma. They detected low-grade dysplasia with a selectivity of 0.93 and a sensitivity of 0.78, and high-grade dysplasia/carcinoma with a specificity and sensitivity of 1. Our group has carried out experiments to classify cellular heterogeneity in glioblastoma multiform (GBM, grade-IV brain cancer) tissue samples (unpublished results). We have used Fourier transform infrared (FTIR) imaging to differentiate between normal and GBM tissue sections. GBMs are known to show large cellular heterogeneity which directly corresponds to the biochemical composition of the tissue. The different cell types studied comprised of fibrillary, pleomorphic, small, giant and lipidized astrocytes. The main aim of the study is to aid pathologists in identification of GBMs, especially in the case of stereotactic biopsies and frozen sections which often lose their morphological identity at low temperature.

Study using model organisms: In order to improve the ability to diagnose and treat human diseases much more efficiently, understanding the mechanism of progression of the disease is necessary, but that would be time-consuming. Therefore, to explore the onset and complexity of various diseases, model organisms are used. A model organism is an animal, plant or microbe that is used to understand a range of biological processes. They should fulfil certain criteria such as short life cycle, easy to breed, maintain in large numbers under laboratory conditions and data generated using these model organisms should be applicable to higher organisms like humans. Mouse, rat, zebrafish, fruitfly, nematode worm, and thale cress are few examples being extensively used for this purpose[17].

The most versatile organism to study diseases in human are the mice, as it shares 99% of their genes with humans. Mice and humans share similarities in most of the physiological and pathological features such as nervous, cardiovascular, endocrine, immune, musculoskeletal and other internal organ systems. There are numerous studies reported in the literature where mice genes have been manipulated in many ways to understand the human physiology[18]. Aiguo *et al.*[19] have shown that Raman spectroscopy is a fast and reliable method to study the liver tissue. They have identified spectral differences between normal mouse liver tissues, and tissues affected by acute alcoholic liver injury and fibrosis *in situ*. They also studied the protection of the liver by indole-3-carbinol (I3C) against acute alcoholic liver damage[19]. Paul *et al.*[20] used the customized fibre-optic probe for *in vivo* assessment of allograft incorporation in a rat model to provide information on the metabolic status of the graft and for early indications of graft success or failure. Toyran *et al.*[21] studied the effect of diabetes on myocardium using FTIR microspectroscopy. They observed changes in lipid and glycogen levels along with a change in the protein profile[21]. Ayca *et al.*[22] studied the most common fungal (disseminated candidiasis) infection in hospitalized patients using the mice model. The study revealed that the infection resulted in changes mainly in lipid profile (ratio of the saturated lipids to unsaturated lipids) and also caused lipid peroxidation[22].

Figure 5 *a* shows the FTIR spectra of mice lungs, spleen and liver tissues recorded by our group, in the

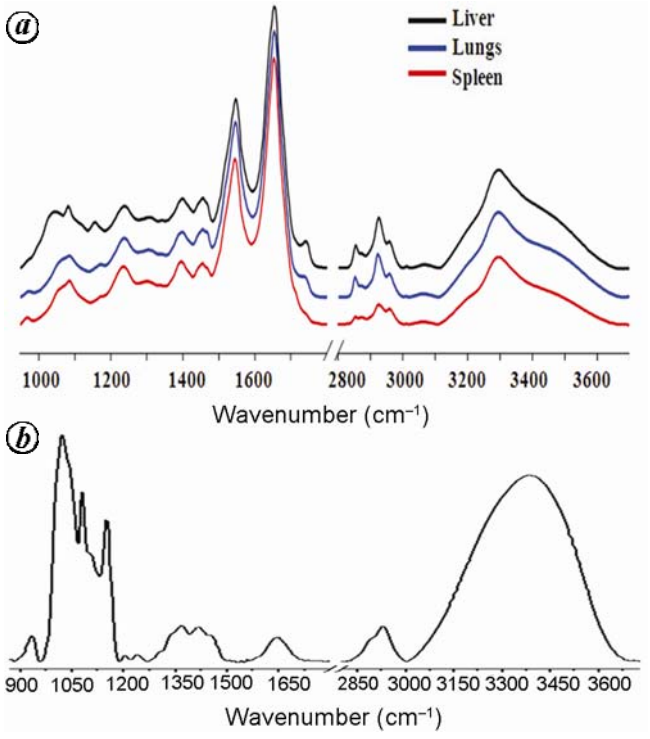

Figure 5. FTIR spectra of (***a***) liver (black), lungs (blue) and spleen (red) tissue from the same mice and (***b***) pure glycogen.

900–3800 cm^{-1} region; the spectra were normalized according to the amide II band. The aim of the study was to characterize different kinds of mice tissues using FTIR microspectroscopy. The FTIR images (FTS 7000 FT–IR spectrometer, UMA 600-IR infrared microscope, Varian) of lungs, spleen and liver were recorded at the resolution of 4 cm^{-1}, and for each image 64 interferograms were co-added. The bands at 1030, 1080 and 1152 cm^{-1} are due to C–O stretching in polysaccharides, symmetric stretching mode of phosphodiester groups in nucleic acids and glycogen, and CO–O–C stretch in polysaccharides respectively. These bands at 1030, 1080 and 1152 cm^{-1} have a strong contribution from glycogen, as demonstrated by the pure glycogen spectrum (Figure 5 *b*). This triad is strong in the case of liver tissue, as the primary function of the liver is glycogen synthesis, storage and breakdown. The ratio of lipids to proteins (2855 cm^{-1}/2873 cm^{-1}), i.e. the ratio of CH_2 symmetric stretching (mainly due to lipids) to the CH_3 symmetric stretching (mainly due to proteins) and the ratio of DNA to RNA, i.e. the ratio C–O stretching mode of deoxyribose to the C–O stretching mode of ribose (966 cm^{-1}/996 cm^{-1}) differs amongst different tissues[23,24]. It shows that the bands arising from the different cellular components like glycogen, proteins, lipids, nucleic acids, etc. are present in all three different types of tissue of the mice. However, depending upon the concentration of various cellular components, the relative intensity of IR bands varies.

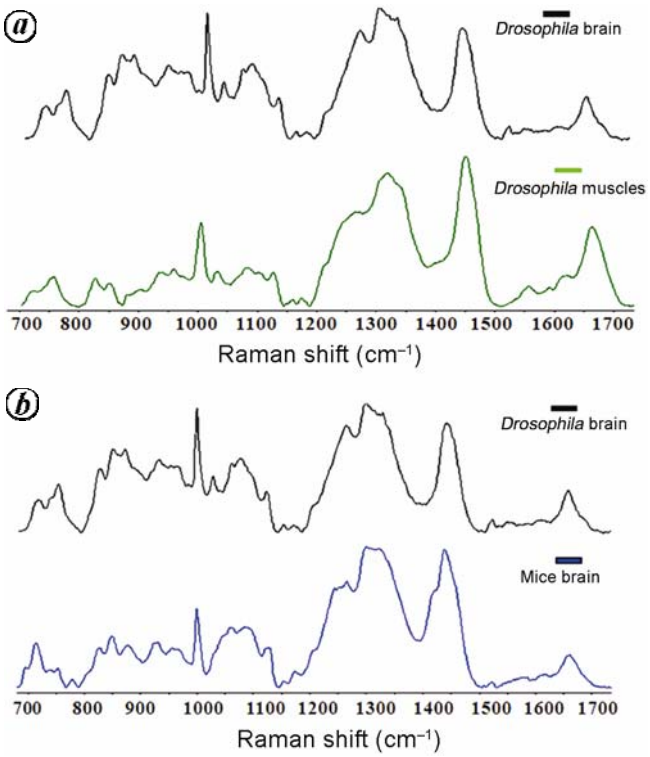

Figure 6. Raman spectra of (***a***) *Drosophila* brain and *Drosophila* muscles, and (***b***) *Drosophila* brain and mice brain.

In addition to mice, we have also used *Drosophila melanogaster* (fruitfly) as a model organism, which has 70% of disease genes similar to disease genes in humans. It has an average life span of 60–70 days, breeds quickly and lays a large number of eggs. Therefore, *Drosophila* provides an opportunity to study age-related human disorders. It plays an important role in understanding genetics and developmental biology[25–27]. *In vivo* label-free imaging of *Drosophila* has been carried out using coherent anti-Stokes Raman scattering[28]. We have carried out some preliminary Raman experiments on the *Drosophila* brain and muscles. The brain was dissected in phosphate buffer saline (PBS), and muscles in 70% ethanol. The samples were mounted on KBr substrate and Raman spectra were recorded with an excitation wavelength of 785 nm (Renishaw, RM 1000; Figure 6). Raman spectra of *Drosophila* brain and muscles were compared under similar experimental conditions.

Effect of surfactant on physico-chemical properties of human hair: Our group has recently reported the effect of surfactants on the physico-chemical properties of human scalp hair using FT–IR ATR spectroscopy, AFM and SEM[29]. Sodium dodecyl sulfate (SDS) was used as the surfactant and conformational changes in the secondary structure of keratin protein present in the outer protective layer of the hair (cuticle) were studied. The effects of such agents have attracted attention from cosmetics manufacturers to improve the quality of their products. Changes in the secondary structure of protein (keratin) were studied by curve-fitting of the amide-I (1641 cm^{-1}) band after sequential SDS treatment. Rearrangements in the protein backbone conformations were observed, wherein post-SDS treatment the β-sheet structure of protein changed in favour of random coil and β-turn structure (Figure 7). AFM and SEM studies allowed us to understand the morphological changes induced due to SDS treatment on the hair surface. AFM and SEM images demonstrated the rupture and partial erosion of superficial sub-layers of hair.

Vibrational spectroscopy of cells, smears, biofluids and biomolecules: Vibrational spectroscopic techniques have been extensively used to understand the various basic processes of life like cell division, cell death via apoptosis or necrosis, differentiation, early diagnosis of diseases, cell–drug interactions, etc. Verrier *et al.*[30] used Raman microspectroscopy for the *in situ* monitoring of apoptosis in lung carcinoma epithelial cells induced by Triton X-100. Specific biochemical changes in proteins, DNA and lipids taking place during the course of cell death were analysed[30]. Cameron *et al.*[31] have carried out a series of experiments on the model and natural membranes in aqueous medium using FTIR spectroscopy to monitor changes occurring in the vibrational pattern of various functional groups as a function of temperature.

Recently, Beier *et al.*[32] have employed confocal Raman microspectroscopy to discriminate between different species of bacteria, which are major components of oral plaque. Confocal Raman microspectroscopy has also been used to assess the mitochondrial status of human spermatozoa. Raman maps helped to understand the effect of UV radiation on different organelles of the sperm[33]. Vibrational spectroscopy has also attracted enormous attention in the field of stem-cell biology[34]. Raman and FTIR microspectroscopic techniques have been used to identify spectral markers to distinguish different cell types derived from the differentiation of mouse embryonic stem cells (mESCs) and human embryonic stem cells (hESCs)[35,36]. A recent study by Lindsay *et al.*[37] has shown the potential of Raman spectroscopy to monitor the formation of a bone-like apatite mineral during the differentiation of human mesenchymal stem cells (hMSCs). Diletta *et al.*[38] have studied embryonic stem-cell differentiation by FTIR spectroscopy to identify the changes during differentiation. As a preliminary step to study biofluids, the spectra of mice serum were recorded by our group using FTIR microspectrometer (FTS 7000, Varian) and FT Raman spectrometer (MultiRAM, Bruker). Figure 8 shows the contrast between the FTIR and FT Raman spectra of dried serum. The C–H stretching modes in the 2850–3050 cm^{-1} spectral region were intense in the Raman spectrum compared to the IR spectrum. However, amide-II band was intense in FTIR spectrum compared to the Raman spectrum. The phenyl-breathing ring of phenylalanine (Phe) at 1002 cm^{-1} is specific to Raman spectrum of biological samples such as cells, tissues, serum, etc.

Cervical cancer detection using vibrational spectroscopy: Cervical cancer is one of the most prevalent cancers among women in developing countries[39]. The WHO Fact Sheet, 2010, reports that 'India has a population of 366.58 million women above the age of 15 years who are at risk of developing cervical cancer'. Current estimates indicate that in India every year 134,420 women are diagnosed with cervical cancer and 72,825 die from the disease. Several factors are responsible for cervical cancer, but the sexually transmitted human papillomavirus (HPV) is the most common cause. Cervical cancer is commonly diagnosed through a Pap smear, complemented by a pelvic examination. Cervical cancer detection using vibrational spectroscopy has been studied by various groups. A summary of these studies has been given in Tables 1 and 2.

Our group has carried out some preliminary IR study on cervical smears. Our objective was to differentiate

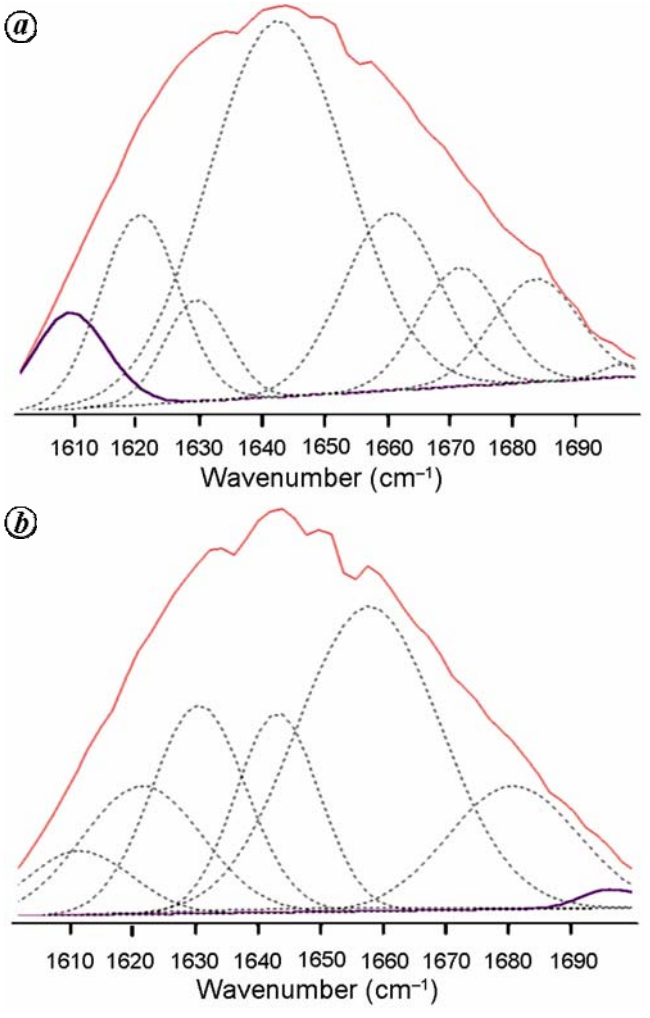

Figure 7. Curve fit spectra of amide I (1600–1700 cm^{-1}) band for (***a***) control root and (***b***) SDS-treated root end of hair.

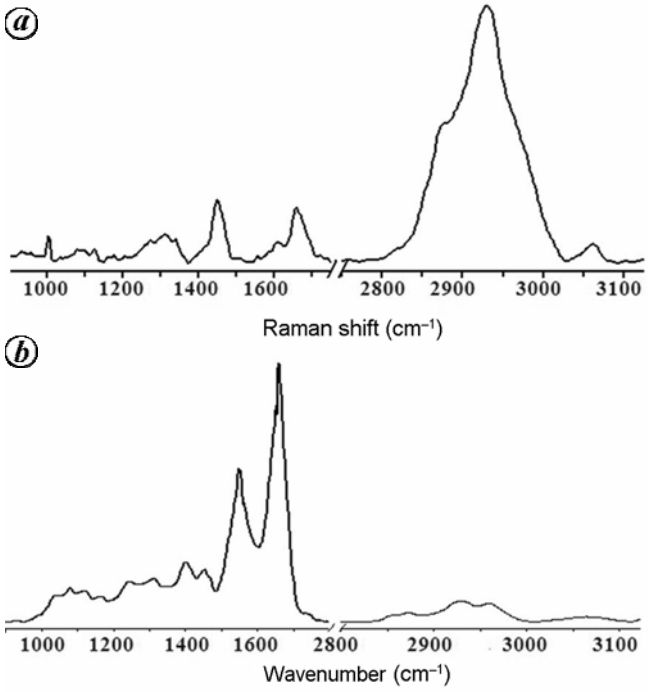

Figure 8. (***a***) FT Raman and (***b***) FTIR spectrum of mice serum.

Table 1. Chronology of advancement in cervical cancer in relation to FTIR spectroscopy

Year and author	Event
1991, Patrick *et al.*	Study of spectroscopic differences between normal, dysplasia and abnormal cervical cells began and the peak assignments were made[59].
1995, Brian *et al.*	Differences between mild and severe dysplasia were found spectroscopically using biopsy sections. Grading of CIN I, CIN II and CIN III was also done[60].
1997, Michael *et al.*	Comparative study between Pap test and FTIR on the basis of specificity, sensitivity, false positives and false negatives was made. Also the biological reasons for changes in peaks were posted[61] (see Table 2).
1997 and 1998, Cohenford and Rigas	Chemometric analysis like PCA was applied on FTIR spectra for the detection of cervical cancer (1997)[62]. Biopsy section analysis using FTIR showed the difference between superficial, intermediate, parabasal, basal and endocervical cells. Two different kinds of spectra for normal cervical section were shown. The differences between the two spectra were the changes in the concentration of glycogen owing to the fact that the basal layer cells are non-dividing and so there is high storage of glycogen, whereas superficial and intermediate cells are highly dividing in nature (1998)[63].
2002, Melissa *et al.*	Benign cellular changes caused by Trichomonas, Candida, Actinomyces, and cellular changes associated with inflammation and atrophy were studied spectroscopically (2002)[64]. Effect of the presence of blood components in cervical smear samples is studied (2002)[65].
1991, Patrick *et al.*	Effect of the presence of polymorphs, debris and other impurities on the IR spectrum was studied. The result showed there were slight differences in intensities of the peak[66].
2003, Ratana *et al.*	Comparative study of cervical cancer with ovarian and endometrial cancers was done[67].
2004, Wood *et al.*	Spectral mapping of various layers of cervical tissue was published[68].
2004 and 2005, Mordechai *et al.*	Apart from glycogen, lipids and proteins, ratio of RNA and DNA was also considered as the spectral biomarker (2004)[69]. Probablistic neural network was applied for FTIR spectrum to distinguish cancer cells (2005)[70].
2007, Walsh *et al.*	Cervical cancer was also analysed using other microspectroscopic techniques like synchrotron radiation IR, ATR, photothermal and Raman[71].
2008, Krishna *et al.*	Potential application of optical spectroscopy like fluorescence, FTIR and Raman was analysed. Raman proved to be a better tool owing to the fact that it does not demand any sample preparation and can be a tool for *in vivo* diagnosis[72].
2011, Mohammadreza and Amir	Since IR holds the following features – non-invasive, rapid, reliable and robust, it has been regarded as the 'green analytical chemistry tool' for cancer detection[73].
2011, Kamila *et al.*	FTIR spectrum was correlated with the $p16^{INK4A}$ expression and HPV copy number, thus reaching the molecular-level detection[74].

Table 2. Comparison between Pap test and FTIR

Method	Sensitivity (%)	Specificity (%)	False negative (%)	False positive (%)
PAP test	86.6	90.5	9.5	13.4
FTIR	98.6	98.8	1.2	1.4

between normal and cancerous smear with minimal pre-processing of the sample. Smear samples were collected from Kidwai Memorial Institute of Oncology, Bangalore, on IR reflective slides and were fixed using 70% ethanol. Smears were imaged using focal plane array detector (64×64 pixels). The IR imaging was carried out in trans-reflection mode at a spectral resolution of 4 cm^{-1}. IR images were frequency colour coded for the 1641 cm^{-1} band. The spectra were baseline-corrected and normalized according to the amide-I band (Origin 6.1, OriginLab). IR spectra of normal and cancerous smears along with the corresponding white light and IR images are shown in Figure 9. Changes observed between normal and cancerous smear spectra have been summarized in Table 3.

Cell–drug interactions: Our group has also been involved in understanding cell–drug interactions, and has carried out a series of IR imaging experiments to probe such interactions. Acetylation and deacetylation of histone proteins are vital for cell function. Acetylation of histones is normally carried out by histone acetyl transferases (HAT), and deacetylation of histones is carried out by histone deacetylase (HDAC) enzymes. HATs and HDACs are mainly responsible for the gene regulation. However, improper function and expression of these enzymes leads to many diseases, including cancer. Histone deacetylase inhibitors (HDIs) are compounds which inhibit the activity of HDAC enzymes and consequently result in acetylation of lysine residues on histones. Using IR microscopy, we have demonstrated that HDIs not only induce acetylation but could also induce propionylation. Introduction of acetyl-specific modification has been indicated by the bands at 2872 and 2960 cm^{-1}, and at 2851 and 2922 cm^{-1}, which originate from stretching vibrations of CH_2 (methylene) groups indicated propionylation[40].

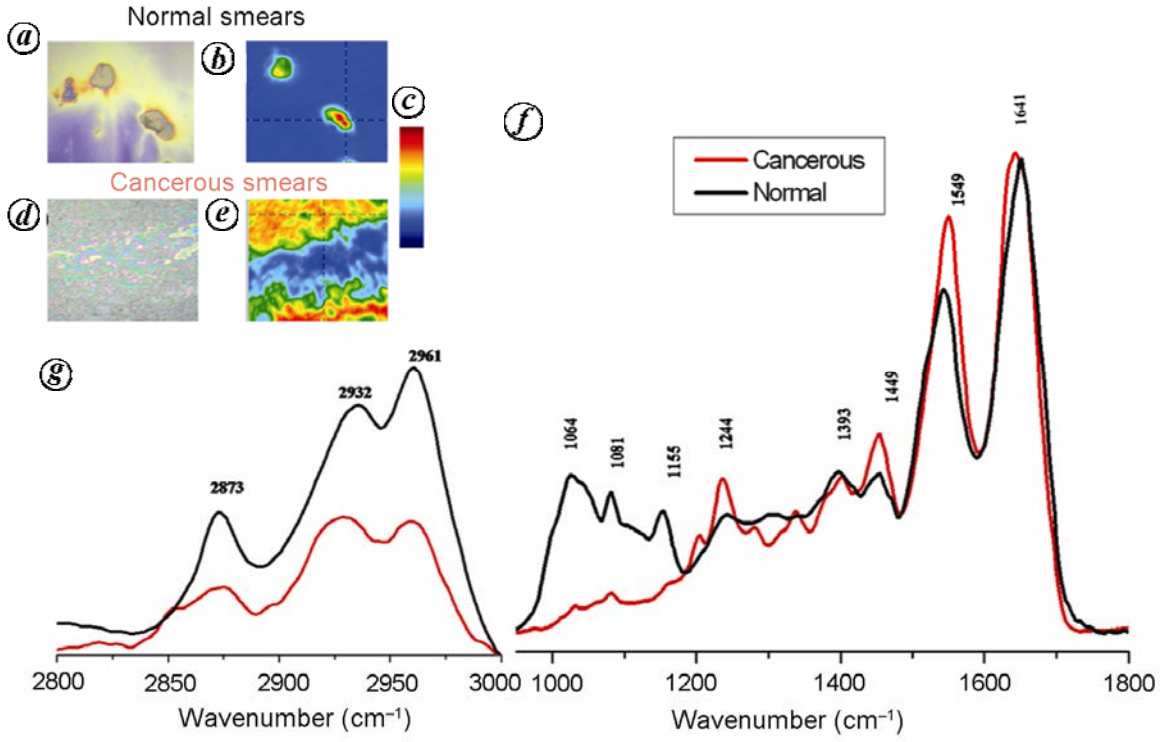

Figure 9. FTIR spectrum of normal and cancerous cervical smear. ***a***, Normal smear white light image; ***b***, Normal smear IR image; ***c***, Colour coding scale; ***d***, Cancerous smear white light image; ***e***, Cancerous smear IR image; ***f***, IR absorbance spectrum from 950 to 1800 cm^{-1}; ***g***, IR absorbance spectrum from 2800 to 3000 cm^{-1}.

Table 3. Discussion about changes in peaks of cervical cancer

Compound	Peak assignments (cm^{-1})	Origin of peaks	Changes observed	Remarks
Glycogen	1025, 1047, 1155 1082 (weak)	C–O stretching and bending from CH_2OH of carbohydrates	Decrease in intensity	Cancer cells use up all the glucose for their fast replication. So there is no storage of excess glucose as glycogen[61].
	1170		Increase in intensity	The intensity of a shoulder band at about 1170 increases in the abnormal cells due to phosphorylation in C–OH groups.
Nucleic acids	1082 and 1244	Phosphate symmetric and asymmetric stretching from nucleic acids	Shift towards higher wave-number	Nuclear compaction reduces in cancer cells due to decrease in hydrogen bonding in DNA leading to increased nucleus/ cytoplasm ratio. Thus absorption energy for stretching increases.
Proteins	1640 (amide I) and 1549 (amide II)	Amide I – stretching C=O (70%) and C–N (30%). Amide II – bending N–H (50%), C–N stretching (40%) and C–C (10%)	Not observed	Since there is not much difference in amide I peak between the normal and cancerous cells, it is taken as the reference for colour coding and normalization.
	1393 and 1449	Symmetric and asymmetric CH_3 bending from amino acid side groups	Ratio of intensity between these two peaks changes	Hypomethylation causes reduction in methyl to methylene ratio[75].
Lipids	2873, 2932 and 2961	C–H stretch from acyl chains of lipids	Intensity ratio changes between 2932 and 2961	Disorder in membrane methylene chains causes the difference between normal and cancer spectra in this region[61].

Applications of Raman and IR microspectroscopy in forensics and pharmaceuticals

Raman and IR spectroscopic techniques have been used for the characterization of drugs and monitoring of the drug-delivery systems[41]. Williams *et al.*[42] have used FTIR microspectroscopy in the field of forensics to analyse the chemistry of the latent fingerprint of children as a function of time and temperature. Presence of three major classes of compounds was shown in the fingerprints: carboxylic acid salts, proteins and esters. FTIR microspectroscopy has also been used as a fast diagnostic technique for the identification of drugs targeting specific molecular pathways causing chronic myeloid leukaemia. Chemometric data analysis was used to assess drug compounds in *ex vivo* cancer cells[43].

Applications of lab-on-a-chip in Raman spectroscopy

Lab-on-a-chip (LOC) is a miniaturized version of an analytical laboratory that performs most of the functions on a single platform. The LOC has various advantages such as minimal sample requirement, reduced analysis time, less wastage and background reduction with reasonable reproducibility. The Raman spectroscopic study using microfluidic devices (LOC) is appealing in certain cases like surface enhanced Raman scattering (SERS)[44–46]. SERS enhances the signal of the probed species placed on or nearby the surface plasmons[47]. In SERS, the sample is adsorbed on a roughened metal surface or nanoparticles, usually of copper, silver or gold. The enhancement observed in SERS spectra is mainly because of two effects: the electromagnetic effect and the chemical effect. Since the observation of this phenomenon in 1974, numerous experiments have demonstrated the applications of SERS in biology, ranging from probing proteins to its applications in *in vivo* microscopy[48–50]. SERS has been useful to detect very low concentrations of drug in human urine samples and to monitor the concentrations of excitatory amino acids like glutamate (Glu) and aspartate (Asp) in the cerebrospinal fluid (CSF), which are indicators of injury in the central nervous system[51]. One of the key concerns with SERS experiments is the reproducibility under similar experimental conditions. It is because nanoparticles tend to aggregate with time and aggregation leads to variable shape and size of SERS substrates, which results in variation in the enhancement behaviour. This limitation can be overcome by performing SERS spectroscopic measurements in flow cells like LOC, which keeps the flow of nanoparticles constant in comparison to conventional SERS[45,46].

To demonstrate the applications of LOC in Raman spectroscopy, spectra of pyridine (0.1 M) using LOC device have been recorded by our group (Figure 10). Experiments were carried out at the excitation wavelength of 514 nm (Renishaw, RM 1000). Silver colloids were synthesized by the reduction of a silver nitrate solution with sodium citrate[52]. Then 1 M KCl solution was used for activation of silver colloids. Pyridine and colloids were introduced into the chip at the same rate (0.038 μl/s), whereas KCl was injected at the rate of 0.020 μl/s and mineral oil was introduced at the rate of 0.833 μl/s. Mineral oil was used to prevent direct contact between the aqueous phase and the microchannel walls. SERS spectra were recorded at the focus point on the LOC (indicated by '∗' in Figure 10).

Chemometrics: application in vibrational spectroscopy

Chemometrics (also called multivariate statistical methods) is defined as the application of mathematical and statistical methods to chemistry and biology[53]. Chemometrics is based on the idea that many non-selective variables must be taken into consideration instead of just one variable, and then ultimately combined in a multivariate model[54]. It basically helps in data analysis, especially in cases where large amounts of data are generated, like in HPLC, NMR, FTIR, Raman and GC-MS. Chemometrics helps researchers to understand and manage the enormous amount of data effectively. The most frequently used chemometric methods in research are factor analysis, principal component analysis (PCA), discriminant analysis, principal component regression, multiple linear regression, cluster analysis and partial least squares regression[55].

Although Raman and IR spectroscopy are powerful techniques for analysing various substances, a significant amount of processing is required to extract useful information from raw spectra. Chemometric methods serve this purpose and have the ability to analyse the vast spectral distribution and thoroughly discriminate between spectra of different samples that show very little changes. Often identification and analysis of components in biological samples by spectroscopic methods alone is difficult because of the diverse nature of the sample[56].

In the case of Raman and IR spectral data, chemometrics helps to improve the understanding of chemical information. Patterns in the data could be modelled and these models can be used routinely to predict the newly acquired data of similar quality. Chemometrics assists in spectroscopic data pre-processing, to reduce and correct interferences such as overlapped band, baseline drifts, scattering and mainly to analyse spectral variations. Spectroscopists mainly use software packages like Matlab, Unscrambler, etc. for data analysis[57]. For example, Robin *et al.*[58] have studied cell-cycle dynamics in single living cells using Raman microspectroscopy, wherein PCA was applied to examine cell cycle-dependent

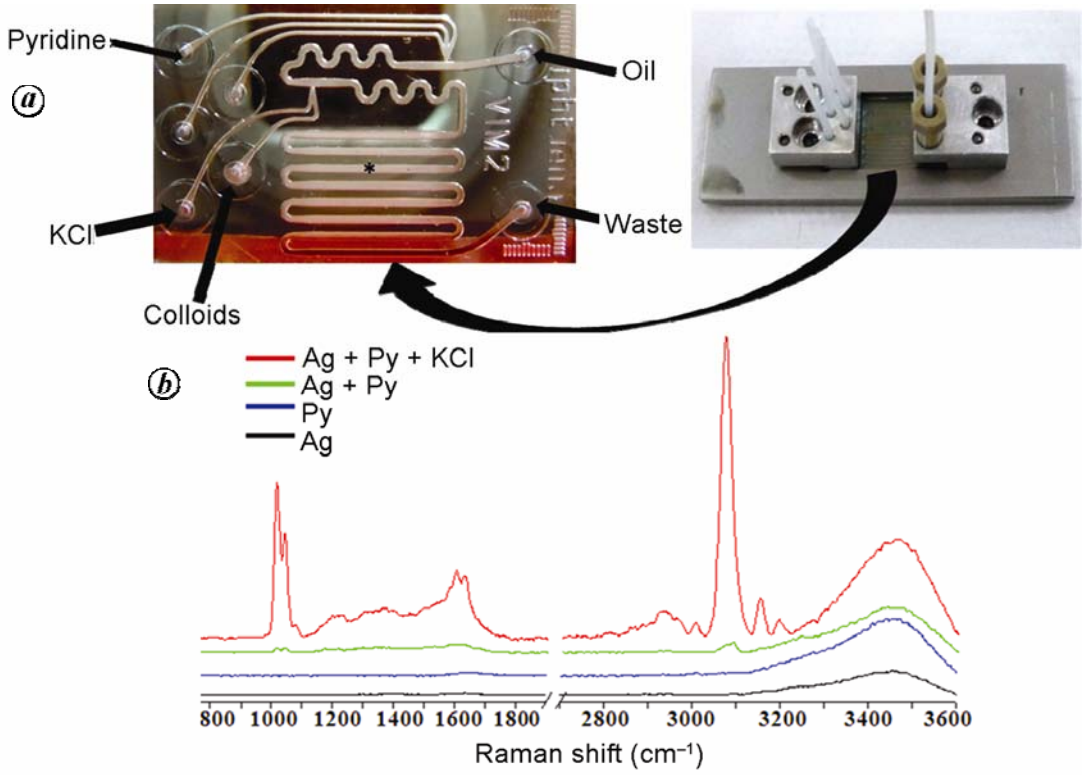

Figure 10. ***a***, Photograph of lab-on-a chip with aluminium holder. ***b***, Raman spectra of silver colloids (Ag; in black), pyridine 0.1 M (Py; blue), silver colloids + pyridine (Ag + Py; in green) and silver colloids + pyridine + KCl 1 M (Ag + Py + KCl; red).

variations in Raman spectral signatures, and linear discriminant analysis as a classification algorithm to differentiate between cells in different phases of the cell cycle. These variations are extremely difficult to observe in raw spectra, thereby necessitating a need for chemometric methods for efficient data analysis and interpretation[58].

Summary

Vibrational microspectroscopic techniques have the potential to diagnose biological samples at the molecular level, as these techniques are sensitive to the changes in the structure, composition and quantity of cellular components. These techniques have demonstrated new opportunities to study individual sub-cellular components, cells, tissues, biofluids, etc. at the molecular level in a non-invasive manner. Furthermore, the spectral and spatial information available at the single-cell level together with chemometric methods has helped in the better understanding of biological processes. The exponential rate of growth in this area over the last few years is a clear indication that Raman and IR microspectroscopic methods would become part of hospital facilities in the near future.

1. Blout, E. R. and Fields, M., Absorption spectra. VII. The infra-red spectra of some nucleic acids, nucleotides, and nucleosides. *J. Biol. Chem*., 1949, **178**, 335–343.
2. Elliott, A. and Ambrose, E. J., Structure of synthetic polypeptides. *Nature*, 1950, **165**, 921–922.
3. Wu, H. W., Volponi, J. V., Oliver, A. E., Parikh, A. N., Simmons, B. A. and Singh, S., *In vivo* lipidomics using single-cell Raman spectroscopy. *Proc. Natl. Acad. Sci. USA*, 2011, **108**, 3809–3814.
4. George, T. and Jacques, C., *Raman Microscopy Developments and Applications*, Academic Press, London, 1996.
5. Peter, R. G. and James, A. de. H., *Fourier Transform Infrared Spectrometry*, Wiley Interscience, Canada, 2007.
6. Prayson, R. A. *et al.*, Interobserver reproducibility among neuropathologists and surgical pathologists in fibrillary astrocytoma grading. *J. Neurol. Sci.*, 2000, **175**, 33–39.
7. Diem, M., Romeo, M., Boydston-White, S., Miljkovic, M. and Matthäus M., A decade of vibrational micro-spectroscopy of human cells and tissue. *Analyst*, 2004, **129**, 880–885.
8. Adele, L. B. and Richard, M., Infrared spectroscopic characterization of mineralized tissues. *Vib. Spectrosc*., 2005, **38**, 107–114.
9. Shan, Y. L., Mei, J. L., Run, C. L. and Shui, M. L., Non destructive analysis of the conformational changes in human lens lipid and protein structures of the immature cataracts associated with glaucoma. *Spectrochim. Acta*, 1998, **54**, 1509–1517.
10. Itte, S., Gijs, F. J. M. V., Kees, O., Gerwin, P. J., Frits, F. M. D. M. and Jan, G., Ageing and changes in protein conformation: a Raman micro-spectroscopic study. *Exp. Eye Res*., 1992, **54**, 759–767.
11. Heraud, P. *et al.*, Early detection of the chemical changes occurring during the induction and prevention of autoimmune-mediated

demyelination detected by FTIR imaging. *Neuroimage*, 2010, **49**, 1180–1189.
12. Yang, T. T. *et al.*, Histopathology mapping of biochemical changes in myocardial infarction by Fourier transform infrared spectral imaging. *Forensic Sci. Int*., 2011, **207**, 34–39.
13. Karen, C. T. *et al.*, Fourier-transform infrared spectroscopy discriminates a spectral signature of endometriosis independent of inter-individual variation. *Analyst*, 2011, **136**, 20–47.
14. Buschman, H. P. *et al.*, Raman microspectroscopy of human coronary atherosclerosis: biochemical assessment of cellular and extracellular morphologic structures *in situ*. *Cardiovasc. Pathol*., 2001, **10**, 69–82.
15. Peter, J. C., Gerald, W. L., Elizabeth, A. C., Hajo, A. B. and Gerwin, J. P., *In vivo* confocal Raman microspectroscopy of the skin: noninvasive determination of molecular concentration profiles. *J. Invest. Dermatol*., 2001, **116**, 434–442.
16. Bakker, T. C. S. *et al*., *In vivo* detection of dysplastic tissue by Raman spectroscopy. *Anal. Chem*., 2000, **72**, 6010–6018.
17. Rachel, A. A. and Sabina, L., What's so special about model organisms? *Stud. Hist. Philos. Sci*., 2011, **42**, 313–323.
18. Nadia, R. and Steve, B., The mouse ascending: perspectives for human-disease models. *Nature Cell Biol*., 2007, **9**, 993–999.
19. Aiguo, S. *et al.*, *In vivo* study on the protection of indole-3-carbinol (I3C) against the mouse acute alcoholic liver injury by micro-Raman spectroscopy. *J. Raman Spectrosc.*, 2009, **40**, 550–555.
20. Paul, I. O., White, F. W. L. E., Steven, A. G. and Michael, D. M., Development of non-invasive Raman spectroscopy for *in vivo* evaluation of bone graft osseointegration in a rat model. *Analyst*, 2010, **135**, 3142–3146.
21. Toyran, N., Lasch, P., Naumann, D., Turan, B. and Severcan, F., Early alterations in myocardia and vessels of the diabetic rat heart: an FTIR microspectroscopic study. *Biochem. J*., 2006, **397**, 427–436.
22. Ayca, D., Kivanc, E., Fatma, B. and Feride, S., Evaluation of disseminated candidiasis on an experimental animal model: a Fourier transform infrared study. *Appl. Spectrosc*., 2007, **61**, 199–203.
23. Magdalena, S. B., Paul, D., Marzena, Z. K., Joanna, C., Marek, L., Dariusz, A. and Anna, K. W., Biomolecular investigation of human substantia nigra in Parkinson's disease by synchrotron radiation Fourier transform infrared microspectroscopy. *Arc. Biochem. Biophys.*, 2008, **459**, 241–248.
24. Chiriboga, L., Yee, H. and Diem, M., Infrared spectroscopy of human cells and tissue. Part VI: a comparative study of histopathology and infrared microspectroscopy of normal, cirrhotic, and cancer liver tissue. *Appl. Spectrosc.*, 2000, **54**, 1–8.
25. Keith, D. B. and Carl, S. T., Diabetic larvae and obese flies – emerging studies of metabolism in *Drosophila*. *Cell Metabol.*, 2007, **967**, 257–266.
26. Lawrence, T. R., Lorraine, P., Sam, C., Michael, G. and Ethan, B., A systematic analysis of human disease-associated gene sequences in *Drosophila melanogaster*. *Genome Res*., 2001, **11**, 1114–1125.
27. Bharucha, K. N., The epicurean fly: using *Drosophila melanogaster* to study metabolism. *Pediatr. Res*., 2009, **65**, 132–137.
28. Cheng, H. C., Wei, W. C., June, T. W. and Ta-Chau, C., Label-free imaging of *Drosophila in vivo* by coherent anti-Stokes Raman scattering and two-photon excitation autofluorescence microscopy. *J. Biomed. Opt.*, 2011, **16**, 016012-1–7.
29. Singh, B. and Umapathy, S., Effect of SDS on human hair: Study on the molecular structure and morphology. *J. Biophoton*., 2011, **4**, 315–323.
30. Verrier, S., Notingher, I., Polak, J. M. and Hench, L. L., *In situ* monitoring of cell death using Raman microspectroscopy. *Biopolymers*, 2004, **74**, 157–162.
31. Cameron, D. G., Casal, H. L. and Mantsch, H. H., The application of Fourier transform infrared transmission spectroscopy to the study of model and natural membranes. *J. Biochem. Biophys. Methods*, 1979, **1**, 21–36.
32. Beier, B. D., Quivey, R. G. and Berger, A. J., Identification of different bacterial species in biofilms using confocal Raman microscopy. *J. Biomed. Opt*., 2010, **15**, 066001-1–5.
33. Konrad, M., Diedrich, A. S., Erik, B. and Martina, H., Confocal Raman microspectroscopy as an analytical tool to assess the mitochondrial status in human spermatozoa. *Analyst*, 2010, **135**, 1370–1374.
34. Vishnu, V. P., Aufried, L., Henk, J. V. M., Vinod, S., Clemens, A. V. B. and Cees, O., Microbioreactors for Raman microscopy of stromal cell differentiation. *Anal. Chem*., 2010, **82**, 1844–1850.
35. Waraporn, T., Kanjana, T., Chanchao, L., Rangsun, P. and Philip, H., Neural differentiation of mouse embryonic stem cells studied by FTIR spectroscopy. *J. Mol. Struct*., 2010, **967**, 189–195.
36. Flavius, C. P., Huey, T. G., Vinoj, G., Chris, D. and Notingher, I., Toward label-free Raman-activated cell sorting of cardiomyocytes derived from human embryonic stem cells. *J. Biomed. Opt*., 2011, **16**, 045002-1–4.
37. Lindsay, L. M., George, A. B., Mura, M. M., Peter, O'H., Mircea, M., Adrian, R. B. and Brian, J. M., Raman spectroscopic monitoring of the osteogenic differentiation of human mesenchymal stem cells. *Analyst*, 2011, **136**, 2471–2481.
38. Diletta, A. *et al.*, Embryonic stem cell differentiation studied by FT–IR spectroscopy. *Biochim. Biophys. Acta*, 2008, **1783**, 98–106.
39. Ahmedin, J., Rebecca, S., Elizabeth, W., Yongping, H., Jiaquan, Xu, Taylor, M. and Michael, J. T., Cancer Statistics, *CA – Cancer J. Clin*., 2008, **58**, 71–96.
40. Singh, B., Sivaraman, B., Somasundaram, K. and Umapathy, S., Fourier transform infrared microspectroscopy identifies protein propionylation in histone deacetylase inhibitor treated glioma cells. *J. Biophoton*., 2012 (in press).
41. Siegfried, W. and Reinhard, H. H. N., Pharmaceutical applications of Mid IR and Raman spectroscopy. *Adv. Drug Deliv. Rev.*, 2005, **57**, 1144–1170.
42. Williams, D. K., Brown, C. J. and Bruker, J., Characterization of children's latent fingerprint residues by infrared microspectroscopy: forensic implications. *Forensic Sci. Int*., 2011, **206**, 161–165.
43. Bellisola, G. *et al.*, Tracking infrared signatures of drugs in cancer cells by Fourier transform IR microspectroscopy. *Analyst*, 2010, **135**, 3077–3086.
44. Michael, K. J. and Thomas, H., Chip devices for miniaturized biotechnology. *Appl. Microbiol. Biotechnol*., 2005, **69**, 113–125.
45. Anne, M., Katrin, R. A., Daniéll, M., Thomas, B., Thomas, H. and Jürgen, P., Towards a quantitative SERS approach – online monitoring of analytes in a microfluidic system with isotope-edited internal standards. *J. Biophoton*., 2009, **2**, 232–242.
46. Katrin, R. S., Dana, C., Petra, R., Thomas, H., Michael, K. and Jurgen, P., A reproducible surface-enhanced Raman spectroscopy approach. Online SERS measurements in a segmented microfluidic system. *Anal. Chem*., 2007, **79**, 1542–1547.
47. Stiles, P. L., Dieringer, J. A., Shah, N. C. and Van Duyne, R. P., Surface-enhanced Raman spectroscopy. *Annu. Rev. Anal. Chem*., 2008, **1**, 601–626.
48. Fleischm, M., Hendra, P. J. and McQuilla, A., Raman-spectra of pyridine adsorbed at a silver electrode. *Chem. Phys. Lett*., 1974, **26**, 163–166.
49. Sebastian, S., SERS microscopy: nanoparticle probes and biomedical applications. *ChemPhysChem*, 2009, **10**, 1344–1354.
50. Wei, X., Penghe, Q. and Chuanbin, M., Bio-imaging, detection and analysis by using nanostructures as SERS substrates. *J. Mater. Chem*., 2011, **21**, 5190–5202.
51. Janelle, M., Reyes, G., Hugh, B. and Nicholas, S., Photodiagnosis using Raman and surface enhanced Raman scattering of bodily fluids. *Photodiagno. Photodyn. Ther*., 2005, **2**, 223–233.

52. Lee, P. C. and Meisel, D., Adsorption and surface-enhanced Raman of dyes on silver and gold sols. *J. Phys. Chem*., 1982, **86**, 3391–3395.
53. Stanley, N. D., Chemometrics: an overview. *Clin. Chem.*, 1986, **32**, 1702–1706.
54. Svante, W., Chemometrics, why, what and where to next. *J. Pharm. Biomed. Anal.*, 1991, **9**, 589–596.
55. Michal, R., Lenka, V. and Eva, P., Application of infrared spectroscopy and chemometric methods for the identification of selected minerals. *Acta Geodyn. Geomater.*, 2011, **8**, 47–58.
56. Rebecca, B. H., Edward, D., Morgan, M. and Frank, V., Fourier transform infrared spectroscopy and improved principal component regression (PCR) for quantification of solid analytes in microalgae and bacteria. *Appl. Spectrosc.*, 2011, **65**, 442–453.
57. Luke, A., Reisner, A. C. and Abhilash, K. P., An integrated software system for processing, analyzing, and classifying Raman spectra. *Chemometr. Intell. Lab.*, 2011, **105**, 83–90.
58. Robin, J. S., Gavin, J. and Molly, M. S., Noninvasive analysis of cell cycle dynamics in single living cells with Raman microspectroscopy. *J. Cell. Biochem*., 2008, **104**, 1427–1438.
59. Patrick, T. T. W. *et al.*, Detailed account of confounding factors in interpretation of FTIR spectra of exfoliated cervical cells. *Proc. Natl. Acad. Sci. USA*, 1991, **88**, 10988–10992.
60. Brian, J. M. *et al.*, Fourier transform infrared spectroscopy of dysplastic, papillomavirus–positive cervicovaginal lavage specimens. *Gynecol. Oncol.*, 1995, **56**, 245–249.
61. Michael, F. K. F., Mary, S., Pascale, E., Wylam, F., Nadia, Z. M. and Patrick, T. T. W., Comparison of Fourier-transform infrared spectroscopic screening of exfoliated cervical cells with standard papanicolaou screening. *Gynecol. Oncol.*, 1997, **66**, 10–15.
62. Cohenford, M. A., Godwin, T. A., Cahn, F., Bhandare, P., Caputo, T. A. and Rigas, B., Infrared spectroscopy of normal and abnormal cervical smears: evaluation by principal component analysis. *Gynecol. Oncol.*, 1991, **66**, 59–65.
63. Cohenford, M. A. and Rigas, B., Cytologically normal cells from neoplastic cervical samples display extensive structural abnormalities on IR spectroscopy: implications for tumor biology. *Proc. Natl. Acad. Sci. USA*, 1998, **95**, 15327–15332.
64. Melissa, J. R., Michael, A. Q., Frank, R. B. and McNaughton, D., Influence of benign cellular changes in diagnosis of cervical cancer using IR microspectroscopy. *Biopolymers*, 2002, **67**, 362–366.
65. Mellisa, J. R., Bayden, R. W., Michael, A. Q. and McNaughton, D., Removal of blood components from cervical smears: implications for cancer diagnosis using FTIR spectroscopy. *Biopolymers*, 2002, **72**, 69–76.
66. Patrick, T. T. W., Rita, K. W., Thomas, A. C., Thomas, A. G. and Basil, R., Infrared spectroscopy of exfoliated human cervical cells: evidence of extensive structural changes during carcinogenesis (cervical cancer/dysplasia/high pressure spectroscopy). *Proc. Natl. Acad. Sci. USA*, 1991, **88**, 10988–10992.
67. Ratana, S. *et al.*, A new approach for the detection of cervical cancer in Thai women. *Gynecol. Oncol.*, 2003, **90**, 10–14.
68. Wood, B. R., Chiriboga, L., Yee, H., Quinn, M. A., Mcnaughton, D. and Diem, M., Fourier transform infrared spectral mapping of the cervical transformation zone, and dysplastic squamous epithelium. *Gynecol. Oncol.*, 2004, **93**, 59–68.
69. Mordechai, S. *et al.*, Possible common biomarkers from FTIR microspectroscopy of cervical cancer and melanoma. *J. Microsc.*, 2004, **215**, 86–91.
70. Podshyvalov, A. *et al.*, Distinction of cervical cancer biopsies by use of infrared microspectroscopy and probabilistic neural networks. *Appl. Opt.*, 2005, **44**, 3725–3734.
71. Walsh, M. J. *et al.*, IR microspectroscopy: potential applications in cervical cancer screening. *Cancer Lett.*, 2007, **246**, 1–11.
72. Krishna, C. M. *et al.*, An overview on applications of optical spectroscopy in cervical cancer. *J. Cancer Res. Ther*., 2008, **4**, 26–36.
73. Mohammadreza, K. and Amir, B. G., Infrared spectroscopy provides a green analytical chemistry tool for direct diagnosis of cancer. *Trends Anal. Chem.*, 2011, **30**, 864–874.
74. Kamila, M. O. *et al.*, Correlation of $p^{16INK4A}$ expression and HPV copy number with cellular FTIR spectroscopic signatures of cervical cancer cells. *Analyst*, 2011, **136**, 1365.
75. Ehrlich, M., Cancer-linked DNA hypomethylation and its relationship to hypermethylation. *Curr. Top. Microbiol. Immunol.*, 2006, **310**, 251–274.

ACKNOWLEDGEMENTS. We thank the Department of Science and Technology (DST) and Department of Biotechnology, Government of India, for financial support. S.U. thanks DST for the J.C. Bose fellowship. B.S. and R.G. thank UGC and CSIR for research fellowships. We also thank Juergen Popp and Anne Maerz for extending their support in the Lab-on-a-chip project.